COMPUTER SIMULATION OF THE NONLINEAR LIQUID-STRUCTURE INTERACTION PROBLEM WITH FREE SURFACE

Al Zeiny
Faculty, Department of Civil & Geomatics Engineering & Construction
California State University, Fresno, CA 93740-8030

PCTEX

ABSTRACT

The dynamic response of liquids has significant influence on the response of civil structures interacting with them. Inappropriate approximation of the liquid motion may lead to major errors in estimating the seismic response of the structure. The liquid pressures and the impact forces form the measurable level of the energy transferred to the structure. In addition, the motion of the structure is the primary source for the liquid energy. Since this energy transfer occurs simultaneously throughout the liquid boundary, it is essential in the finite element analysis of such problems to use a model that effectively deals with the coupling between the liquid and the structure.

Preprint

INTRODUCTION

The equations of motion of a liquid may be formulated by two different approaches, corresponding to the two ways in which the problem of determining the motion of a liquid mass, acted on by given forces and subjected to given boundary conditions, may be viewed. The Eulerian formulation is obtained by considering the object of our investigations to be the knowledge of the velocity, pressure and density at all points of space occupied by the liquid for all instances. On the other hand, the Lagrangian form is obtained by considering the object to be the determination of the history of each particle. Detailed discussions of the two forms may be found in [5]. In the current investigation, a Lagrangian description of the structure's motion is utilized, which makes it necessary to use a Lagrangian description of the liquid-structure interface in order to enforce compatibility between the structure and liquid elements. The continuity equation in the Eulerian form is utilized inside the liquid domain to mathematically simulate the liquid motion.

The liquid in this analysis is considered to be inviscid, irrotational and incompressible. Such assumptions are true for most of civil structures interacting with liquids. These assumptions allow displacements, pressures or velocity potentials to be the variables in the liquid domain. The displacement-based liquid elements may be easy to incorporate in finite element programs for structural analysis and simplify the enforcement of the liquid-structure interface constraints. However, such elements require two or three degrees of freedom per node. In addition, this approach is not well suited for problems with large liquid displacements and requires special care to prevent zero-energy rotational modes from arising. Alternatively, using pressures or velocity potentials as the unknown degrees of freedom requires only one degree of freedom per node inside the liquid domain, which significantly reduces the computational cost of the analysis, and adequately represent the physical behavior of the liquid. The latter approach is used in this investigation.

VARIATIONAL PRINCIPLES OF THE GENERAL LIQUID-STRUCTURE INTERACTION PROBLEM

In general, liquid-structure interaction may be divided into five categories. Each category requires specific formulation and unknowns that may not be suitable for others. As shown in Figure (1), category five is characterized by the free surface existence, which combines the sloshing phenomenon with the liquid-structure interaction. The free surface may also be viewed as a structure boundary for the liquid, but with zero stiffness. Since this structure boundary can not take any force, the liquid pressure has to be eliminated on this boundary in order to fulfill the equilibrium conditions. The virtual work statement used to describe the nonlinear general liquid structure interaction in civil structures is developed in this section. Figure (2) shows the general geometry of a liquid sloshing in a container. The structure is modeled using appropriate structural elements. The formulation presented in this section is independent of the structure. This property of the current formulation allows it to be used in the analysis of any general liquid-structure interaction problem.

Preliminary Evaluation

Structural Domain

Following Hamilton's principle, the energy function for the structure domain may be written as

$$\begin{aligned}\Pi_s &= \int_{t_1}^{t_2} \left[\frac{1}{2} \int_{\Omega_s} \boldsymbol{\epsilon}^T \mathbf{E}\, \boldsymbol{\epsilon}\, d\Omega_s - \frac{1}{2} \int_{\Omega_s} \rho_s \dot{\mathbf{u}}^T \dot{\mathbf{u}}\, d\Omega_s \right. \\ &- \left. \int_{\Gamma_w} \mathbf{u}^T \mathbf{f}^I\, d\Gamma_w - \int_{\Omega_s} \mathbf{u}^T \mathbf{f}^E\, d\Omega_s \right] dt \end{aligned} \tag{1}$$

where $\mathbf{E}$ is the stress-strain matrix, $\boldsymbol{\epsilon}$ is the strain vector, $\mathbf{u}$ is the displacement vector, Ω_s is the structural domain, Γ_w is the wet surface of the structure, $\mathbf{f}^I$ is the liquid pressure vector, $\mathbf{f}^E$ is the body force vector and ρ_s is the mass density of the structure. Setting variations on Π_s to zero gives the principle of virtual displacements

$$\begin{aligned}\delta\Pi_s = \int_{\Omega_s} \delta\boldsymbol{\epsilon}^T \mathbf{E}\, \boldsymbol{\epsilon}\, d\Omega_s &+ \int_{\Omega_s} \rho_s \delta\mathbf{u}^T \ddot{\mathbf{u}}\, d\Omega_s - \int_{\Gamma_w} \delta\mathbf{u}^T \mathbf{f}^I\, d\Gamma_w \\ &- \int_{\Omega_s} \delta\mathbf{u}^T \mathbf{f}^E\, d\Omega_s = 0 \end{aligned} \tag{2}$$

Liquid Domain

The variational indicator of an incompressible liquid flowing under gravity field is obtained by subtracting the kinetic energy from the potential energy of an infinitesimal element of volume $d\Omega_f$, then integrating over the liquid domain Ω_f, which yields

$$\Pi_f = \int_{t_1}^{t_2} \left[\int_{\Omega_f} \left\{ \rho_f g y - \frac{1}{2} \rho_f \mathbf{V}.\mathbf{V} \right\} d\Omega_f \right] dt \tag{3}$$

where ρ_f is the mass density of the liquid, y is the Cartesian coordinate measured in a direction opposite to that of the gravitational acceleration g, and $\mathbf{V}$ is the velocity vector. The continuity condition and the kinematic condition are still need to be enforced on the

liquid domain. The kinematic condition insures that the normal liquid velocity at the liquid boundary matches the rate of normal displacement of the boundary. Using Lagrange multipliers, the two conditions are added to the variational indicator as follows

$$\Pi_f = \int_{t_1}^{t_2} \left[\int_{\Omega_f} \left\{ \rho_f g y - \frac{1}{2} \mathbf{V}.\mathbf{V} - \lambda_1 \rho_f \bigtriangledown \mathbf{V} \right\} d\Omega_f + \int_{\Gamma_f} \lambda_2 \left\{ v_n - \dot{u}_n \right\} d\Gamma_f \right] dt \tag{4}$$

where λ_i refers to the ith Lagrange Multiplier, $\dot{u}_n$ is the time derivative of the normal displacement of the boundary and v_n is the normal velocity at the liquid boundary. Taking variations with respect to $\mathbf{V}$ gives the following Euler-Lagrange equations

$$\delta \mathbf{V} : \qquad -\rho_f \mathbf{V} + \rho_f \bigtriangledown \lambda_1 = 0 \qquad \text{in } \Omega_f \tag{5}$$

$$\delta v_n : \qquad \lambda_2 - \rho_f \lambda_1 = 0 \qquad \text{on } \Gamma_f \tag{6}$$

Thus,

$$\mathbf{V} = \bigtriangledown \lambda_1 \tag{7}$$

$$\lambda_2 = \rho_f \lambda_1 \tag{8}$$

It is evident from Equation (7) that physically λ_1 is the scalar velocity potential. Therefore, Equation (4) may be rewritten as

$$\Pi_f = \int_{t_1}^{t_2} \rho_f \left[\int_{\Omega_f} \left\{ g y - \frac{1}{2} \bigtriangledown^2 \phi - \phi \bigtriangledown^2 \phi \right\} d\Omega_f + \int_{\Gamma_f} \phi \left\{ \frac{\partial \phi}{\partial \mathbf{n}} - \dot{u}_n \right\} d\Gamma_f \right] dt \tag{9}$$

After integrating by parts, Equation (9) may be rewritten as

$$\Pi_f = \int_{t_1}^{t_2} \rho_f \left[\int_{\Omega_f} \left\{ g y + \frac{1}{2} \bigtriangledown^2 \phi + \dot{\phi} \right\} d\Omega_f \right] dt \tag{10}$$

or concisely,

$$\Pi_f = \int_{t_1}^{t_2} \left[\int_{\Omega_f} P d\Omega_f \right] dt \tag{11}$$

where P is the total pressure which may be also written as

$$P = P_o - \gamma_f \left[\frac{1}{g} \frac{\partial \phi}{\partial t} + \frac{\bigtriangledown \phi . \bigtriangledown \phi}{2g} + y \right] \tag{12}$$

where P_o is the hydrostatic pressure at the point.

PCTEA Evaluation

Coupled Liquid-Structure System

In order to apply the variational principle to the liquid-structure interaction problem, the liquid and the structure functionals, given by Equations (1) and (10), are combined together. The two statements are coupled at the liquid-structure interfaces by

$$u_n = \frac{\partial \phi}{\partial \mathbf{n}} \tag{13}$$

$$\mathbf{f}^I = P\,\mathbf{n} \tag{14}$$

where $\mathbf{n} = (n_x, n_y, n_z)$ is the outward normal unit vector from the liquid towards the structure.

PCTEX

FINITE ELEMENT DISCRETIZATION

The development of the liquid element that is capable of modeling the liquid behavior when interacting with flexible structures is achieved throughout several stages. First, the classical isoparametric liquid element, which is also used to model the liquid motion inside the liquid domain, is developed. Then, the element is enhanced with the nonlinear sloshing and liquid-structure interaction in order to model the liquid boundaries.

Evaluation

Isoparametric Liquid Element Formulation

The strong form of the steady state velocity potential flow of incompressible liquid may be stated as follows:
Given $v_n(\mathbf{x}) : \Gamma_f \rightarrow \mathbf{R}$ find $\phi(\mathbf{x}) : \Omega_f \rightarrow \mathbf{R}$ such that

$$\text{Continuity Condition:} \qquad \rho_f \bigtriangledown^2 \phi(\mathbf{x}) = 0, \qquad \forall\ \mathbf{x} \in \Omega_f \tag{15}$$

$$\text{Kinematic Condition:} \qquad \frac{\partial \phi}{\partial \mathbf{n}} = v_n, \qquad \forall\ \mathbf{x} \in \Gamma_f \tag{16}$$

where v_n is the prescribed normal velocity across the liquid boundaries. This strong form yields the following variational equation

$$\rho_f \int_{\Omega_f} \bigtriangledown(\delta\phi)\ \bigtriangledown\phi\ d\Omega_f = \rho_f \int_{\Gamma_f} \delta\phi\ v_n\ d\Gamma_f \tag{17}$$

Following the classical isoparametric finite element discretization, the following relations are obtained;

$$\mathbf{K}_f = \rho_f \int_{\Omega_f} \mathbf{B}_f^T \mathbf{B}_f\ d\Omega_f \tag{18}$$

$$\mathbf{F}_{int} = \rho_f \int_{\Omega_f} \mathbf{B}_f^T \mathbf{V}_f\ d\Omega_f \tag{19}$$

$$\mathbf{F}_{ext} = \rho_f \int_{\Gamma_f} \mathbf{N} v_n \, d\Gamma_f \tag{20}$$

$$= \rho_f \int_{\Gamma_f} \begin{bmatrix} N_1N_1 & N_1N_2 & \dots \\ N_2N_1 & N_2N_2 & \dots \\ \vdots & \vdots & \ddots \end{bmatrix} d\Gamma_f \begin{Bmatrix} v_{n1} \\ v_{n2} \\ \vdots \end{Bmatrix} \tag{21}$$

$$= \mathbf{M}_f^j \tag{22}$$

$$[D_f] = \begin{bmatrix} \frac{\partial N_1}{\partial x} & \frac{\partial N_2}{\partial x} & \dots \\ \frac{\partial N_1}{\partial y} & \frac{\partial N_2}{\partial y} & \dots \\ \vdots & \vdots & \ddots \end{bmatrix} \tag{23}$$

$$\{V_f\} = \bigtriangledown\phi = \mathbf{B}_f\Phi \tag{24}$$

where $\mathbf{K}_f$ is the liquid stiffness matrix, $\mathbf{F}_{int}$ and $\mathbf{F}_{ext}$ are the liquid internal and external flow vectors, respectively, $\mathbf{V}_f$ is the liquid velocity vector, Φ is the nodal velocity potential vector, j is the liquid element edge number that is subjected to a normal discharge of speed v_n, $\mathbf{M}_f^j$ is the liquid element mass matrix for edge number j and N_i is the ith isoparametric shape function. Physically, $\mathbf{F}_{ext}$ is the nodal discharge vector entering or leaving the element domain as a result of the normal velocity of the liquid across the liquid domain boundaries. This natural boundary condition ensures the normal velocity compatibility at the liquid boundaries (kinematic condition). The tangential velocity does not contribute to the discharge vector and consequently will have no effect on the continuity equation. $\mathbf{F}_{int}$ is the internal discharge vector resulting from the current gradient of the velocity potential function, ϕ. The continuity equation is satisfied when $\mathbf{F}_{int}$ and $\mathbf{F}_{ext}$ are in equilibrium. The residual discharge is then given by

$$\mathbf{R}_f = \mathbf{F}_{ext} - \mathbf{F}_{int} \tag{25}$$

This residual is mainly caused by the free surface motion and the consequent remeshing of the liquid domain. This yields to an iterative modified Newton-Rapson scheme in the form

$$[K_f]\{\delta\phi\}_i = \{R_f\}_i \tag{26}$$

The vector $\delta\Phi_i$ is then used to correct the velocity potential vector after the ith iteration.

Nonlinear Liquid Sloshing in Rigid Structures

Liquid sloshing is defined to be the free surface gravity waves caused by an excitation to a liquid domain. Figure (3) shows the geometry of the problem of liquid sloshing in a rigid structure. In the special case of rigid structures, the translational motion of the liquid boundaries are directly proportional to the ground excitation. The normal velocity of the boundaries is then given by

PCTA Evaluation

$$\mathbf{V}(\mathbf{x},t) = \dot{\mathbf{G}} + \begin{bmatrix} 0 & r_z & -r_y \\ -r_z & 0 & r_x \\ r_y & -r_x & 0 \end{bmatrix} \begin{Bmatrix} \dot{\theta}_x \\ \dot{\theta}_y \\ \dot{\theta}_z \end{Bmatrix} \tag{27}$$

$$v_n(\mathbf{x},t) = \mathbf{V}.\mathbf{n} \tag{28}$$

where $\mathbf{n}$ is the normal to the liquid boundary, (r_x, r_y, r_z) is the position vector of a generic point on the liquid boundary, $\dot{\mathbf{G}}$ is the ground translation velocity vector and $(\dot{\theta}_x, \dot{\theta}_y, \dot{\theta}_z)$ is the ground rotational velocity vector. In plane problems, Equation (27) is reduced to

$$\mathbf{V}(\mathbf{x},t) = \dot{\mathbf{G}} + \begin{Bmatrix} -r_y \\ r_x \end{Bmatrix} \dot{\theta}_z \tag{29}$$

The strong form of the boundary value problem that represent the nonlinear liquid sloshing problem with rigid structure boundaries is stated as follows:
Given $v_n(\mathbf{x},t) : \Gamma_w \times [0,T] \rightarrow \mathbf{R}$, the initial free surface Γ_{so}, and the initial conditions of the potential function $\phi_o(\mathbf{x}) : \Omega_f \rightarrow \mathbf{R}$, find $\phi(\mathbf{x},t) : \overline{\Omega}_f \times [0,T] \rightarrow \mathbf{R}$ and $\Gamma_s \times [0,T] \rightarrow \mathbf{R}$ such that

Continuity Condition:	$\nabla^2 \phi(\mathbf{x},t) = 0$	$\forall \ \mathbf{x} \in \overline{\Omega}_f$	(30)
Initial Conditions:	$\phi(\mathbf{x},0) = \phi_o(\mathbf{x})$,	$\forall \ \mathbf{x} \in \Omega_f$	(31)
	$\Gamma_s(0) = \Gamma_{so}$		(32)
Kinematic Condition:	$\frac{\partial \phi}{\partial \mathbf{n}} = v_n$,	$\forall \ \mathbf{x} \in \Gamma_w$	(33)
Dynamic Condition:	$\frac{\partial \phi}{\partial t} = -\frac{\nabla^2 \phi}{2} - gh$,	$\forall \ \mathbf{x} \in \Gamma_s$	(34)
Kinematic Condition:	$\frac{\partial \phi}{\partial y} = \frac{\partial h}{\partial t} + \frac{\partial \phi}{\partial x}\frac{\partial h}{\partial x} + \frac{\partial \phi}{\partial z}\frac{\partial h}{\partial z}$,	$\forall \ \mathbf{x} \in \Gamma_s$	(35)

where Γ_s is the free surface boundary, Γ_w is liquid boundary in contact with the structure and h is the free surface elevation. Equation (34) represents the dynamic condition that comes from prescribing the pressure value at the free surface in Bernulli's equation, while Equation (35) represents the kinematic condition that enforces the vertical velocity compatibility between the free surface and the liquid domain.

As a result of the simplified assumptions, lack of viscosity sometimes causes undesirable contribution from the high frequency components in the numerical solution of the problem. This contribution is undesirable because of the high frequency modes in the solution that are poorly represented in the discritized system. Any wave that has a length shorter than the element width is not represented adequately due to the limited order of the shape functions. As a result, dispersion error may develop in the solution of some problems. This occurs, sometimes, when the liquid is in the resonance zone or when the excitation level is relatively high. Numerical dissipation may be used then to damp out the high frequency wave components propagating near the free surface. A numerical dissipation term was suggested by Chen [1] for the two-dimensional solution of the problem. He reported that this term has

Preview Evaluation

a little effect on the low frequency modes that govern the solution. After incorporating the numerical dissipation, Equation (35) may be rewritten in the two-dimensional case as

$$\frac{\partial \phi}{\partial y} + \nu_x \frac{\partial^2 h}{\partial x^2} = \frac{\partial h}{\partial t} + \frac{\partial \phi}{\partial x}\frac{\partial h}{\partial x} \tag{36}$$

where ν_x is the damping parameters given as function of the mesh density, l_x, and the wave convection speed relative to the mesh $\mathbf{V}_r$ as

$$\nu_x = \mu \frac{l_x}{2} |V_{rx}| \tag{37}$$

where l_x is taken as the width of the liquid element below the free surface in the x direction and μ is a parameter varies between 0 and 1 to tune the damping globally. In addition, the simplified assumptions, sometimes, causes physical instability of the numerical solution used when the free surface slope is very steep, 70° to 80°. This is attributed to the wave breaking phenomenon which is not incorporated into the current model. This is very likely to occur when the liquid is in the resonance zone, e.g. Figure (14), or when the excitation level is relatively high, e.g. Figure (15).

In case of large amplitude surface waves, it is desirable to update the mesh to follow the liquid boundaries and to avoid distorted elements. In such a case, the time derivatives of any spatial function should be modified to account for mesh speed according to the following relation

$$\frac{\partial F}{\partial t} = \frac{\partial f}{\partial t} - \mathbf{V}_m \cdot \nabla f \tag{38}$$

where $\mathbf{V}_m$ is the mesh speed and F is the function defined with respect to the fixed coordinate system while f is the function defined with respect to the moving mesh.

Discrete Finite Element Implementation: Discrete finite element implementation is achieved by enhancing the isoparametric element developed in Section to model large amplitude free surface liquid sloshing. This is performed by enforcing the nonlinear dynamic and kinematic conditions given by Equations (34) and (35) directly on each of the free surface nodes iteratively, as follows

$$(R_d)_i = \rho_f A_i \left(\frac{\partial \phi}{\partial t} + \frac{\nabla^2 \phi}{2} + gh \right)_i \tag{39}$$

$$(R_k)_i = \rho_f A_i \left(\frac{\partial h}{\partial t} + \frac{\partial \phi}{\partial x}\frac{\partial h}{\partial x} + \frac{\partial \phi}{\partial z}\frac{\partial h}{\partial z} - \frac{\partial \phi}{\partial y} \right)_i \tag{40}$$

where A_i is the liquid free surface node tributary area projected in the horizontal plane, h is the free surface elevation, and $(R_d)_i$ and $(R_k)_i$ are the residuals corresponding to the dynamic and the kinematic equations at the node after iteration i, respectively. Physically, R_d represent the pressure force applied at the free surface node due to violation of the

PCTFT Evaluation

dynamic condition, while R_k is the discharge vector at the free surface node resulting from violating the kinematic condition. At equilibrium, the global residual vector of the entire system should be zero, which means that both the dynamic and kinematic conditions are satisfied at the free surface nodes. Taking the first variation of R_k and R_d gives, after linearization, the following modified Newton-Rapson Iterative scheme at each free surface node

$$\begin{bmatrix} 0 & \rho_f A_i \\ \rho_f A_i & 0 \end{bmatrix} \begin{Bmatrix} \delta\dot{\phi} \\ \delta\dot{h} \end{Bmatrix} + \begin{bmatrix} 0 & 0 \\ 0 & \rho_f A_i g \end{bmatrix} \begin{Bmatrix} \delta\phi \\ \delta h \end{Bmatrix} = \begin{Bmatrix} R_k \\ R_d \end{Bmatrix} \tag{41}$$

It should be pointed out that the variation of the liquid velocity and free surface slopes are ignored in Equation (41). This linearized version of the iterative scheme yields a symmetric coefficient matrix on the left hand side, however, it requires few more iterations to satisfy equilibrium. Although nonlinear schemes may be faster to converge, but they produce a nonsymmetric coefficient matrix on the left hand side, which requires almost double of the symmetric storage and computational cost.

Continuous Finite Element Implementation: Continuous finite element implementation is achieved by working directly from the variational indicator. In order to derive the virtual work statements to be discretized, the variations of Equation (40) with respect to ϕ and u_n are taken, thus

$$\delta\phi: \qquad \rho_f \int_{\Omega_f} \nabla(\delta\phi)\, \nabla\phi\, d\Omega_f - \rho_f \int_{\Gamma_f} \delta\phi\, \dot{u}_n\, d\Gamma_f = 0 \tag{42}$$

$$\delta u_n: \qquad \int_{\Gamma_s} P\delta u_n\, d\Gamma_s = 0 \tag{43}$$

Equation (42) may be rewritten as

$$\delta\phi: \qquad \rho_f \int_{\Omega_f} \nabla\, (\nabla\phi)\ \delta\phi\, d\Omega_f - \rho_f \int_{\Gamma_f} \delta\phi\ \left(\dot{u}_n - \frac{\partial\phi}{\partial\mathbf{n}}\right)\ d\Gamma_f = 0 \tag{44}$$

Since the virtual variables are arbitrary, the Euler equations that govern the liquid behavior are

$$\text{Continuity Condition:} \qquad \nabla^2\phi = 0 \quad \text{on } \Omega_f \tag{45}$$

$$\text{Kinematic Condition:} \qquad \dot{u}_n = \frac{\partial\phi}{\partial\mathbf{n}} \quad \text{on } \Gamma_f \tag{46}$$

$$\text{Dynamic Condition:} \qquad P = 0 \quad \text{on } \Gamma_s \tag{47}$$

Equation (46) represents the kinematic condition at the liquid-structure interface Γ_w and at the free surface Γ_s. On the other hand, Equation (47) represents the dynamic condition only at the free surface Γ_s because u_n is considered as unknown only at the free surface.

pCTFX Evaluation

Linearization of Equations (42) and (43) is achieved by assuming that the free surface elevation h is equal to the normal displacement of the free surface u_n and ignoring the term $\nabla^2\phi$ in Equation (12), this yields to

$$\begin{bmatrix} 0 & \mathbf{M}_f^j \\ \mathbf{M}_f^j & 0 \end{bmatrix} \begin{Bmatrix} \delta\dot{\Phi} \\ \delta\dot{\mathbf{h}} \end{Bmatrix} + \begin{bmatrix} 0 & 0 \\ 0 & g\mathbf{M}_f^j \end{bmatrix} \begin{Bmatrix} \delta\Phi \\ \delta\mathbf{h} \end{Bmatrix} = \begin{Bmatrix} \mathbf{R}_k \\ \mathbf{R}_d \end{Bmatrix} \tag{48}$$

$$\mathbf{R}_d = \mathbf{M}_f^j \left\{ \frac{\partial\phi}{\partial t} + \frac{\nabla^2\phi}{2} + gh \right\} \tag{49}$$

$$\mathbf{R}_k = \mathbf{M}_f^j \mathbf{v}_n - \rho_f \int_\Omega \mathbf{B}_f^T \mathbf{V}_f \, d\Omega \tag{50}$$

where j is the free surface edge number, $\mathbf{V}_f$ is the liquid velocity vector and $\mathbf{v}_n$ is the normal velocity vector at free surface nodes. The normal velocity at a free surface node i is computed as

$$v_{ni} - \mathbf{n}_i^T \begin{Bmatrix} V_x \\ \dot{h} \\ V_z \end{Bmatrix}_i \tag{51}$$

where $\mathbf{n}_i$ is the normal vector to the free surface at the node, and V_x and V_z are the velocity of free surface node i in the x and z direction due to the mesh speed, respectively.

Nonlinear Liquid Sloshing in Flexible Structures

The modified Newton-Rapson method is used to solve the nonlinear system of equations. The left hand side of the system represent the tangent coefficient matrix, while the right hand side represent the residual vector. Most elements have contribution to both sides. In this section, the contribution of the liquid-structure interaction element to both sides is presented.

On the Right Hand Side: As shown in Figure (4), a structure node, in contact with the liquid domain, is subjected to the liquid pressure and, at the same time, delivers energy to the liquid. Since the liquid mesh is updated after each iteration to comply with the new free surface shape and deformed boundaries of the structure, the liquid nodes are moving with respect to the structure nodes. A geometric analysis, similar to what need to be performed in contact analysis, is applied on liquid and structure nodal coordinates and displacements to determine which liquid element is in contact with the current structure node. The normal velocity compatibility condition at liquid-structure interfaces gives

$$\dot{u}_n - \frac{\partial\phi}{\partial\mathbf{n}} \tag{52}$$

This condition causes an external discharge vector to be applied on the liquid element due to the normal velocity of the structure boundary. Hence,

PCTH Evaluation

$$\mathbf{F}_{ext} = \rho_f \int_{\Gamma_w^f} \mathbf{N}\, d\Gamma_w^f \;\; \mathbf{n}^T \dot{\mathbf{u}} \tag{53}$$

where Γ_w^f is the liquid element surface in contact with the structure and $\mathbf{N}$ is the shape function vector for the element nodes located on that surface. The dynamic condition at liquid-structure interfaces requires that the liquid pressure be integrated and applied on the structure node, which gives

$$\mathbf{F}^I = \int_{T_a} P\, \mathbf{n}\, dT_a = T_a\, P\, \mathbf{n} \tag{54}$$

where T_a is the tributary area served by the structure node and P is the total pressure at the structure node given by Equation (12).

On the Left Hand Side: Invoking the variation of Equation (53) gives

$$\delta\mathbf{F}_{ext} = \rho_f \int_{\Gamma_w^f} \mathbf{N}\, d\Gamma_w^f\, \mathbf{n}^T\, \delta\dot{\mathbf{u}} \tag{55}$$

while invoking the variation of equation (54) provides

$$\delta\mathbf{F}^I = T_a\, \mathbf{n}\, \delta P \tag{56}$$

$$= T_a\, \mathbf{n}\, \delta\left(P - \rho_f\left[\frac{\partial\phi}{\partial t} + \frac{\nabla\phi.\nabla\phi}{2g} + y\right]\right) \tag{57}$$

which after linearization gives

$$\delta\mathbf{F}^I = T_a\, \rho_f\, \mathbf{n}\, \delta\dot{\Phi} = T_a\, \rho_f\, \mathbf{n}\, \mathbf{N}^T\, \delta\dot{\Phi} \tag{58}$$

Equation (55) simulates the effect of small change in the structure degrees of freedom on the liquid discharge vector, while Equation (58) simulates the effect of small change in the liquid degrees of freedom on the pressure force vector applied on the structure. Therefore, the liquid-structure coupling matrix is given as

$$\mathbf{C}_{fs} = \rho_f \int_{\Gamma_w^f} \mathbf{N}\, d\Gamma_w^f \;\; \mathbf{n}^T \tag{59}$$

while the structure-liquid coupling matrix is given as

$$\mathbf{C}_{sf} = T_a\, \rho_f\, \mathbf{n}\, \mathbf{N}^T \tag{60}$$

In order to achieve symmetric equations, the liquid-structure coupling matrix should be equal to the transpose of the structure-liquid coupling matrix. For this to be so, to satisfy this condition, one states

PCTEX
Evaluation

$$T_a \mathbf{N} = \int_{\Gamma_w^f} \mathbf{N} \, d\Gamma_w^f \tag{61}$$

which could be easily maintained by choosing the finite element mesh of both the liquid and the structure domains on the interface to posses the following properties

1. The tributary area served by the structure node coincide with the liquid element edge in contact with the structure, i.e. $T_a = \Gamma_w^f$
2. The structure node location is chosen such that the shape function vector of the fluid element at the structure node equals to the vector that consists of the ratios of the surface area served by each fluid node to the total surface area in contact with the structure, i.e. the following relation is satisfied

$$T_a \, \mathbf{N}_{\text{At the structure node location}} = \frac{1}{\rho_f} \mathbf{M}_f^j \, \mathbf{I} \tag{62}$$

where j is the liquid element edge in contact with the structure node and $\mathbf{I}$ is a unit column. For example, in case of linear shape functions, the structure node should be in the middle of the liquid element face, as shown in Figure (4).

In case of large amplitude free surface waves, the mesh is updated to follow the liquid boundaries. This makes it impossible to maintain the symmetry conditions. One or more structure nodes may be located along the same liquid element edge and in positions that violate the symmetry conditions. In this case the closest structure node to the symmetric position is chosen and $\mathbf{C}_{fs}$ is used to couple the liquid element with this structure node only. This technique is found to produce good quadratic convergence. Although using nonsymmetric matrices may be faster to converge, it requires almost double of the symmetric storage and computational cost. The developed approach is found to be convenient and efficient.

The global right hand side is then given as

$$\begin{bmatrix} \mathbf{M}_s & \mathbf{0} & \mathbf{0} \\ \mathbf{0} & \mathbf{0} & \mathbf{0} \\ \mathbf{0} & \mathbf{0} & \mathbf{0} \end{bmatrix} \begin{Bmatrix} \delta\ddot{\mathbf{u}} \\ \delta\ddot{\Phi} \\ \delta\ddot{\mathbf{h}} \end{Bmatrix} + \begin{bmatrix} \mathbf{C}_s & \mathbf{C}_{fs}^T & \mathbf{0} \\ \mathbf{C}_{fs} & \mathbf{0} & \mathbf{C}_{\phi h} \\ \mathbf{0} & \mathbf{C}_{\phi h}^T & \mathbf{0} \end{bmatrix} \begin{Bmatrix} \delta\dot{\mathbf{u}} \\ \delta\dot{\Phi} \\ \delta\dot{\mathbf{h}} \end{Bmatrix} + \begin{bmatrix} \mathbf{K}_s & \mathbf{0} & \mathbf{0} \\ \mathbf{0} & \mathbf{K}_f & \mathbf{0} \\ \mathbf{0} & \mathbf{0} & \mathbf{K}_h \end{bmatrix} \begin{Bmatrix} \delta\mathbf{u} \\ \delta\Phi \\ \delta\mathbf{h} \end{Bmatrix} \tag{63}$$

where $\mathbf{C}_{\phi h}$ and $\mathbf{K}_h$ are the matrices resulting from the assembly of either Equation (41) or Equation (48), and $\mathbf{h}$ is the free surface elevation degrees of freedom vector.

It should be pointed out that the developed liquid-structure interaction implementation could be also used to handle the nonlinear sloshing problem. The liquid free surface could be treated as a liquid-structure boundary on which the structure has zero stiffness. In order to fulfill the equilibrium condition, the liquid pressure has to be eliminated on this boundary.

Preview

COMPUTER IMPLEMENTATION AND TESTING

The formulation of the nonlinear sloshing problem and the liquid-structure interaction are incorporate into DYNAZ [2], the nonlinear multi-system-analysis finite element code. The developed liquid element uses selective uniform integration techniques. It also allows the use of variable nodes to accommodate wide variety of problems and to allow for appropriate mesh refinements. Several cases are then tested and compared with previous investigations.

Two-Dimensional Examples

Example 1- Linear Response to Sinusoidal Ground Excitation: A rectangular tank of 10 m. width and 10 m. liquid height was tested for small ground excitation. The excitation has 6.16 second period and given by

$$\dot{G}_x = 0.01 \sin t \ \text{m/sec}$$

Two finite element meshes are used - one consists of 10×10 liquid elements while the other consists of 20×20 elements. Figure (5) shows a comparison of the liquid response to the ground excitation with the analytical solution using the linear wave theory presented in [1]. Figure (6) shows the effect of the mesh density on the linear liquid response.

Example 2- Nonlinear Response to Mexico City Earthquake: A rectangular tank of 30 ft. width and 15 ft. liquid height is subjected to the North West component of the Mexico City earthquake, shown in Fig (13) in the period domain. This particular liquid height to base ratio $H/2R = 0.5$ was reported as the ratio that is most affected by the nonlinear sloshing effect. The peak ground acceleration of this component of Mexico City earthquake is $0.168g$. The liquid has a specific gravity of 62.4 lb/ft^3. In order to filter high frequency surface wave components that propagate along the free surface, a dissipation factor of 0.75 is used. A finite element mesh that consists of 20×20 4-noded isoparametric liquid elements with a total of 441 nodes is used. Results are obtained and compared to those obtained from Ref. [1]. Figures (7) and (8) show wave height time history along the tank left and right wall, respectively. Figures (9) (10) show the free surface profile at two different time instants. Figures (11) and (12) show the base shear and overturning moments applied on the tank walls and base plate due to the hydrodynamic pressure, respectively.

Example 3- Free Surface Wave Breaking Due to Resonance: A rectangular tank of 12 ft. width and 12 ft. liquid height is subjected to the North West component of the Mexico City earthquake. The earthquake, shown in Fig (13) in the period domain, is found to posses strong components of period range between 1.9 and 3.0 seconds with its maximum at period 2.05 second. Using the linear analytical solution presented in [1], the liquid fundamental period is computed as follows

$$\begin{aligned} \alpha_1 &= \frac{\pi}{2R} = 0.262 \\ \omega_1 &= \sqrt{\alpha_1 g \tanh(\alpha_1 H)} = 2.898 \ \text{rad/sec} \\ T_1 &= 2.168 \ \text{sec.} \end{aligned}$$

Since the free surface sloshing fundamental period is within the range of the strong components of the ground excitation, the free surface wave is expected to break. As expected, it is observed that the free surface wave breaks at time 61.8 seconds, as shown in Fig (14).

Example 4- Free Surface Wave Breaking Due to High Level of Excitation: A rectangular tank of 10 ft. width, 10 ft. liquid height and 2 inches wall thickness is subjected to a sinusoidal ground excitation given by

$$\ddot{G}_x = 1.0g\cos(3.81t)$$

Since the level of excitation is relatively high, the liquid is expected to respond violently to the strong high frequency vibrations delivered to the liquid throughout the tank walls. As expected, the free surface wave breaks at time 4.0 seconds, as shown in Fig (15).

Three-Dimensional Examples

Example 5- Linear Response of an Anchored Liquid Storage Tank: The linear response of a cylindrical liquid storage tank to the Channel 3:360 corrected record of the Northridge earthquake measured at Arleta cite which has a peak ground acceleration of $0.344g$, was found. The finite element mesh is used is shown in Figure (16). The tank has 37 ft. diameter, 32 ft. height, 28.3 ft. liquid height, 3/8 in. wall thickness, and 1/2 in. base plate and roof thickness. Results were compared to those obtained from the analysis presented in reference [4]. Figure (17) shows the time history response of the horizontal acceleration of the tank shell top node. Figure (18) shows shell base axial stress time history. Figure (19) shows shell hoop stress time history at 25% of the shell height measured from the bottom of the tank. Figures (20) and (21) show the tank base shear and base overturning moment time histories due to pressure on tank wall, respectively.

Example 6- Simulation of Nonlinear Seismic Response of Concrete Arch Dam: DYNAZ was used to model the Big Tujunga concrete arch dam, its impounded reservoir and its rock foundation as shown in Fig (22). The tank is constructed as cantilever monoliths separated by contraction joints. During seismic events, these contraction joints open and close altering the transfer of internal forces between arch and cantilever actions. Results are comparable to those obtained from [3].

CONCLUSION

A numerical method has been presented in order to solve the three-dimensional non-linear fluid-structure interaction problem. The presented $\phi - U$ formulation provides an excellent alternative to displacement-based finite element programs. The approach is easy to implement in displacement-based finite element programs and requires much less number of degrees of freedom in the fluid. In addition, the presented $\phi - U$ formulation produces a symmetrical fluid-structure interaction matrix, which is more efficient in both storage and computations.

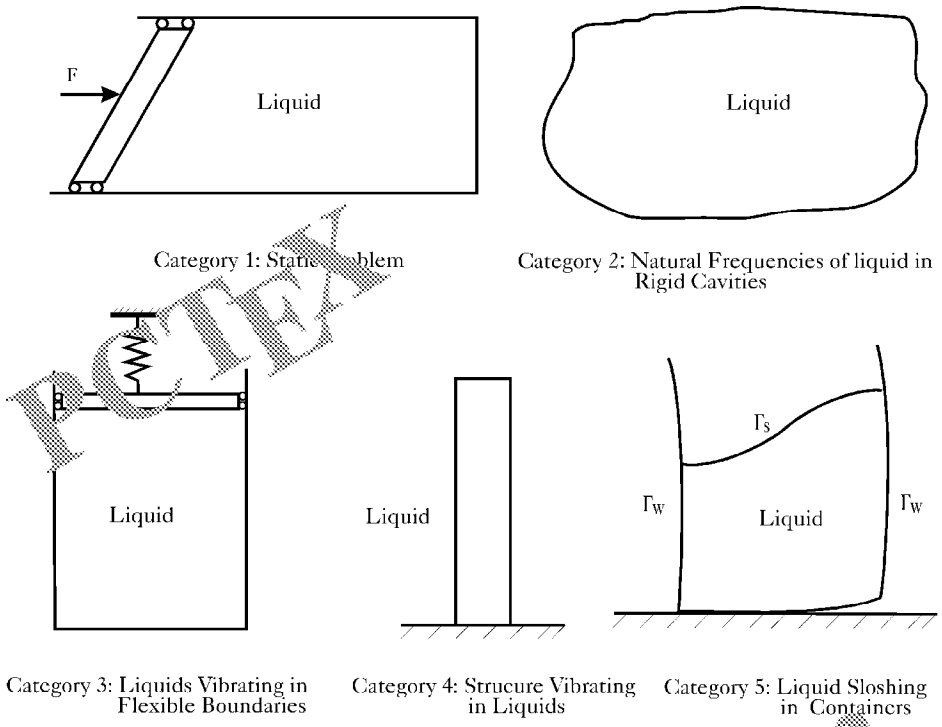

Category 1: Static Problem

Category 2: Natural Frequencies of liquid in Rigid Cavities

Category 3: Liquids Vibrating in Flexible Boundaries

Category 4: Strucure Vibrating in Liquids

Category 5: Liquid Sloshing in Containers

Figure 1: Categories of the Liquid-Structure Interaction Problems

PCTEX
Evaluation

REFERENCES

References

[1] Chen, W., "Nonlinear Liquid Sloshing Motion in Seismically-Excited Rectangular Tanks", Ph.D. Dissertation, University of California, Irvine, 1993.

[2] El-Zeiny, A.A., "Nonlinear Time-Dependent Seismic Response of Unanchored Liquid Storage Tanks", Ph.D. Dissertation, Department of Civil and Environmental Engineering, University of California, Irvine, 1995.

[3] Fenves, G., and Soheil, M., "ADAP-88 : a Computer Program for Nonlinear Earthquake Analysis of Concrete Arch Dams", Earthquake Engineering Research Center, University of California, Berkeley. Report No. UCB/EERC-89-12, 1989.

[4] Haroun, M.A., "arthquake Response of Deformable Liquid Storage Tank", Journal of Applied Mechanics, ASME, Vol. 48, No. 2, June, 1981, pp. 411-418.

[5] Lamb, H., Hydrodynamics, 6th Edition, Dover Publications, New York, 1945.

PCTEX

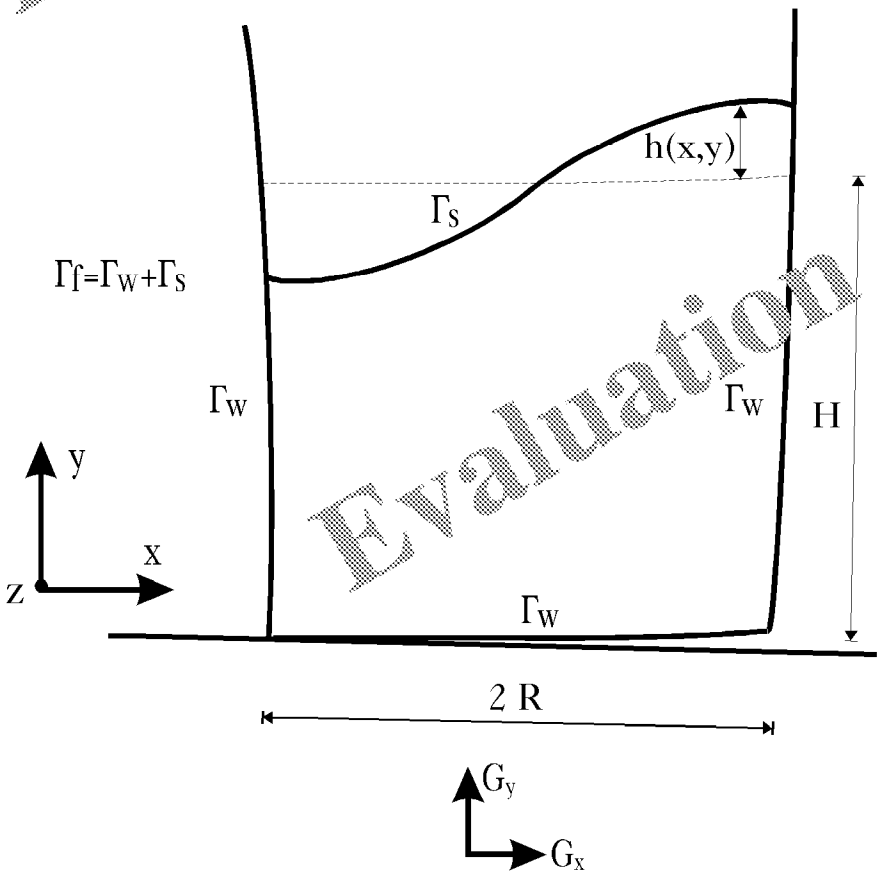

Evaluation

Figure 2: Geometry of the Nonlinear Liquid Sloshing in Flexible Structures

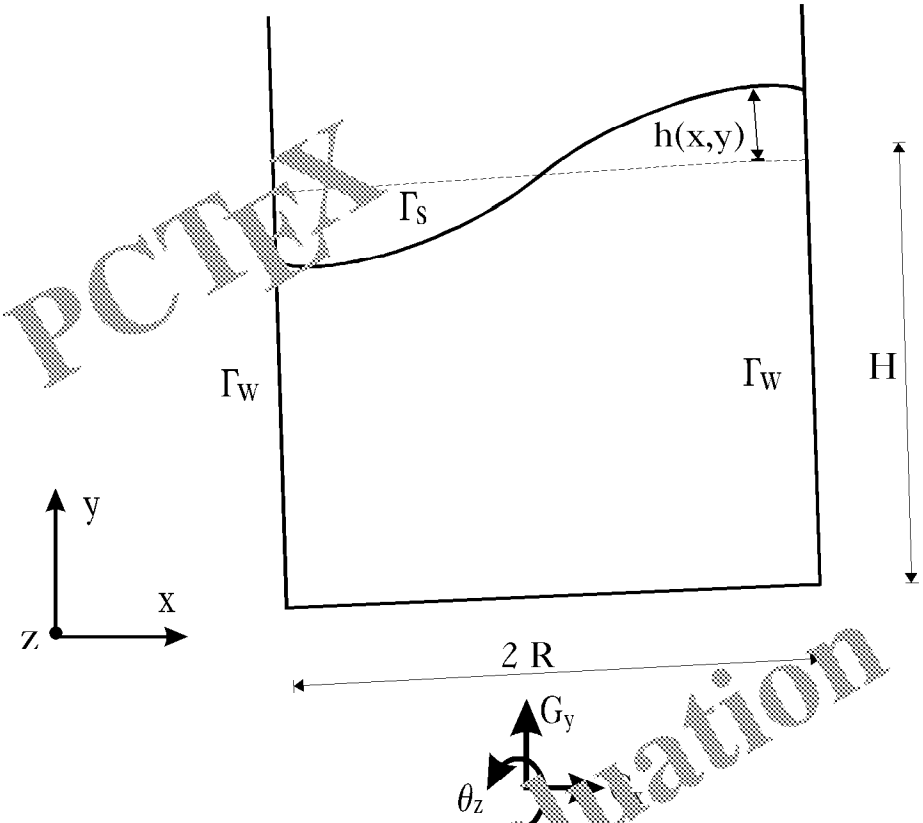

PCTEX Evaluation

Figure 3: Geometry of the Nonlinear Liquid Sloshing Problem with Rigid Structure Boundaries

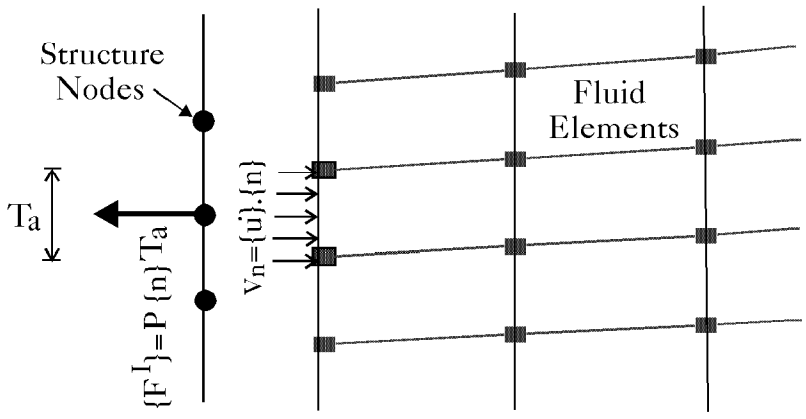

Figure 4: Boundary Conditions at a Structure Node in Contact with a Liquid Element

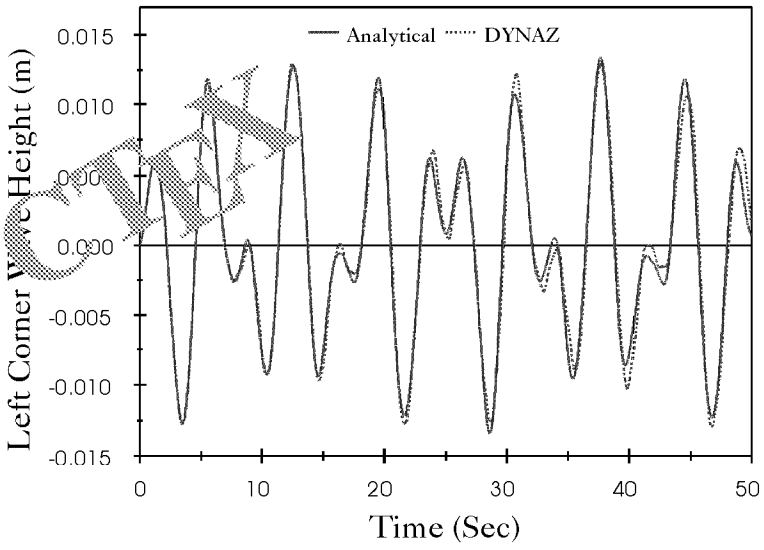

Figure 5: Example 1, Comparison with the Analytical Solution of the Linear Wave Theory.

PCTEF
Evaluation

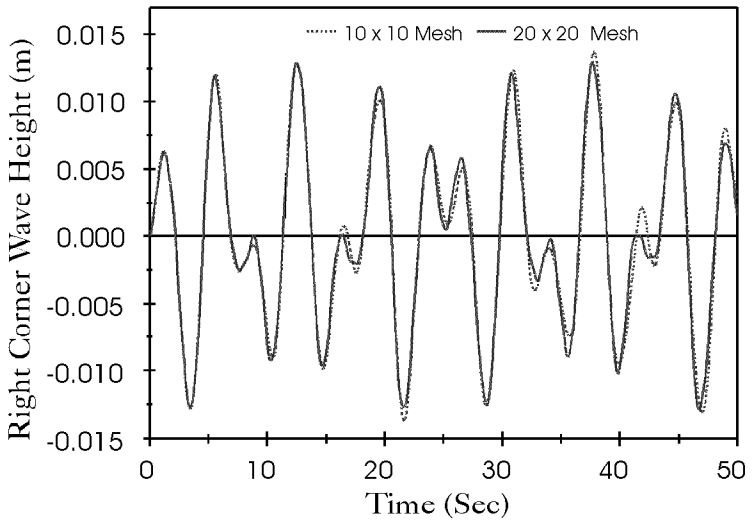

Figure 6: Example 1, Effect of Mesh Density on the Response.

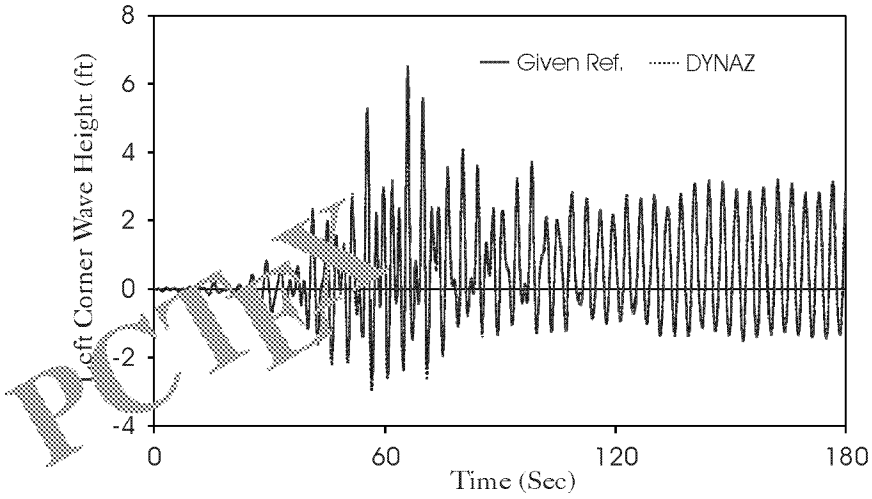

Figure 7: Example 2, Wave Heights at Left Corner

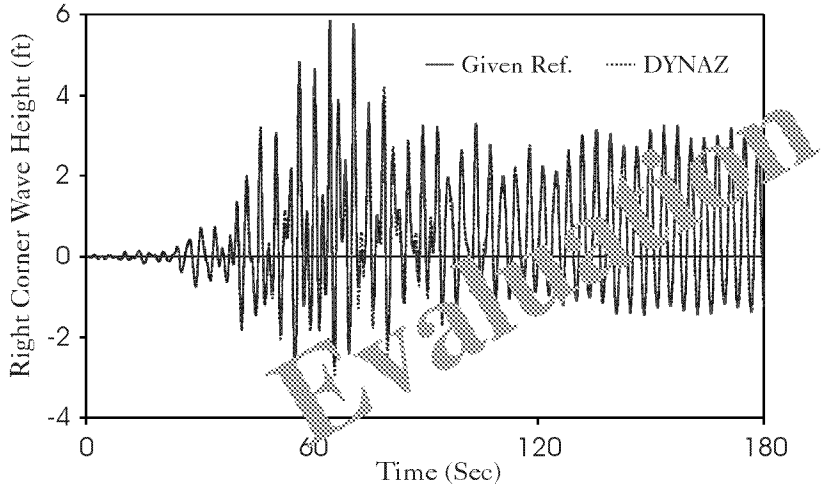

Figure 8: Example 2, Wave Heights at Right Corner

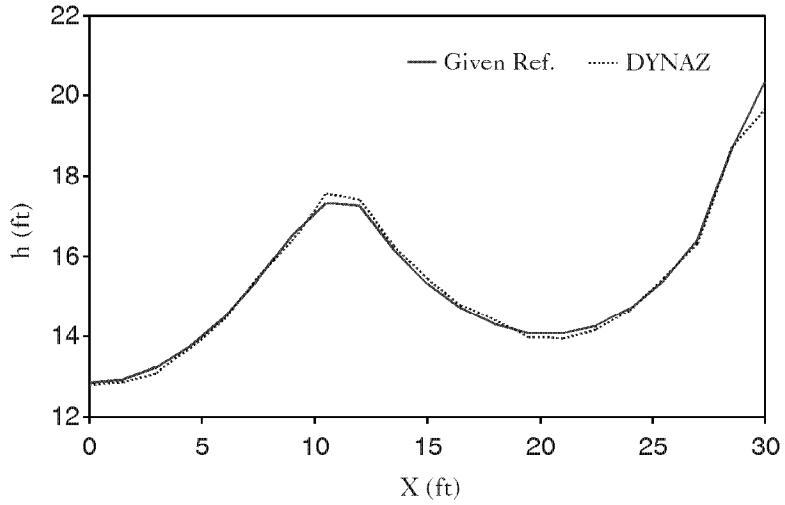

Figure 9: Example 2, Free Surface Profile at Time $t = 65.0$ sec

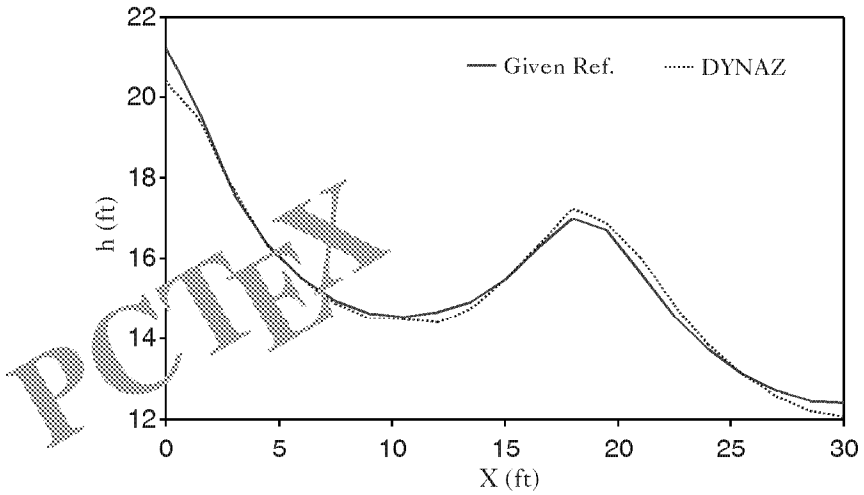

Figure 10: Example 2, Free Surface Profile at Time $t = 66.1$ sec

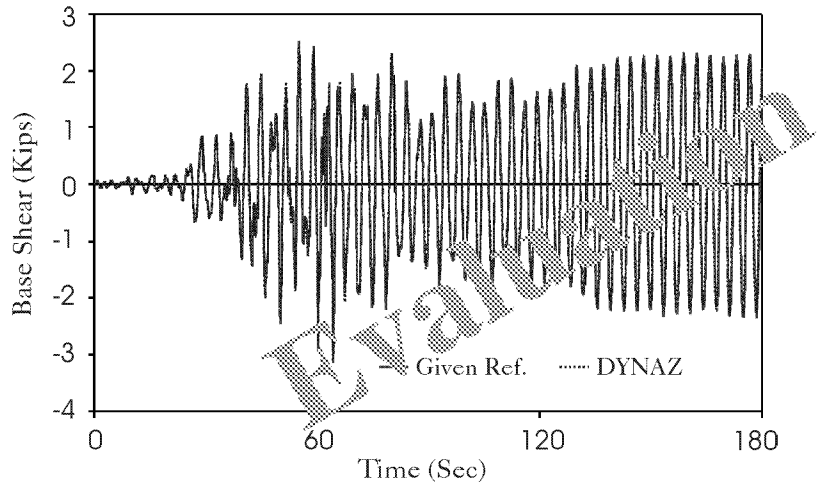

Figure 11: Example 2, Base Shear

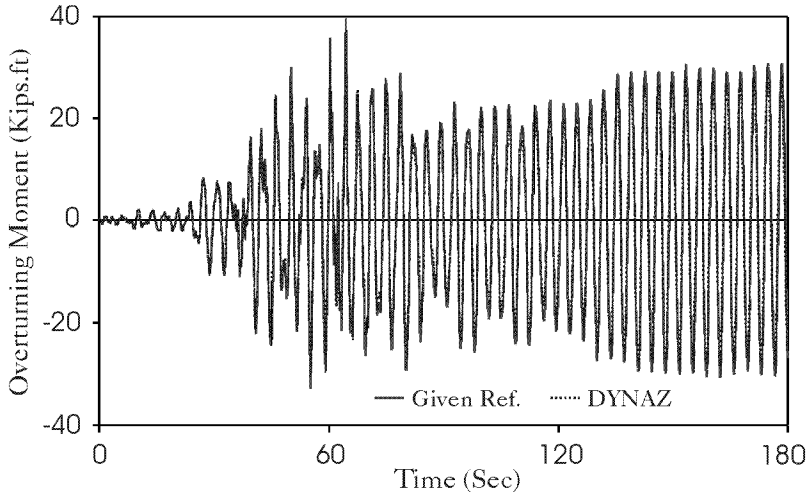

Figure 12: Example 2, Base Overturning Moment

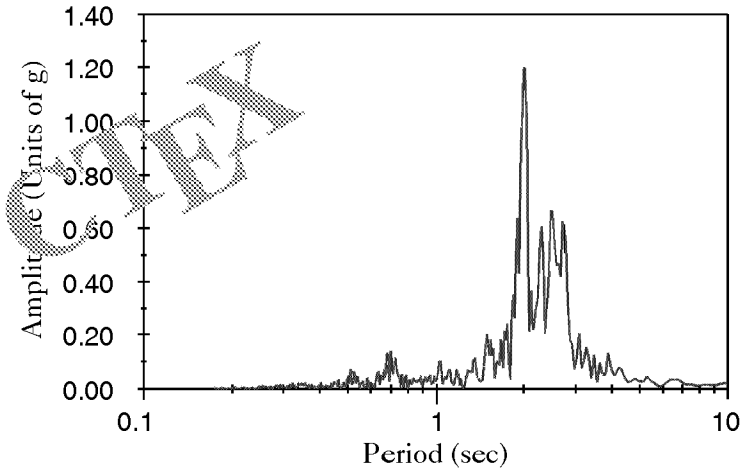

Figure 13: Example 3, Period Content of the Mexico City Earthquake, NW-Component

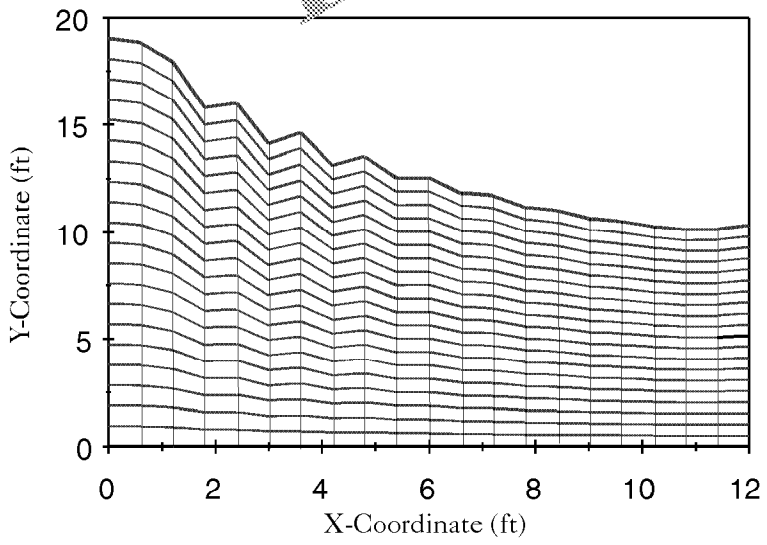

Figure 14: Example 3, Liquid Domain Just Before the Free Surface Wave Breaks

PCFEX
Evaluation

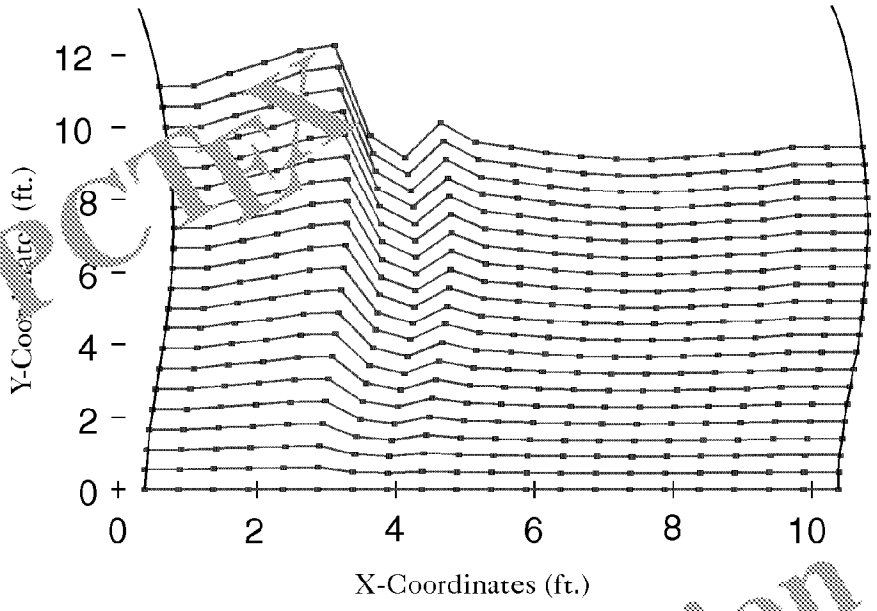

Figure 15: Example 4, Liquid Domain Just Before the Free Surface Wave Breaks

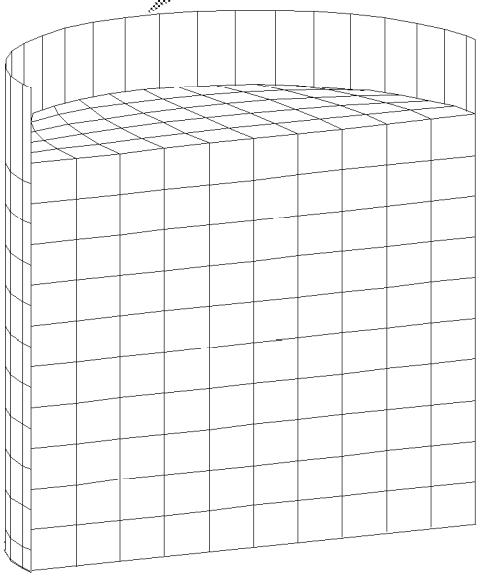

Figure 16: Example 5, Finite Element Mesh of the Coupled Liquid-Tank System

PCTEST
Evaluation

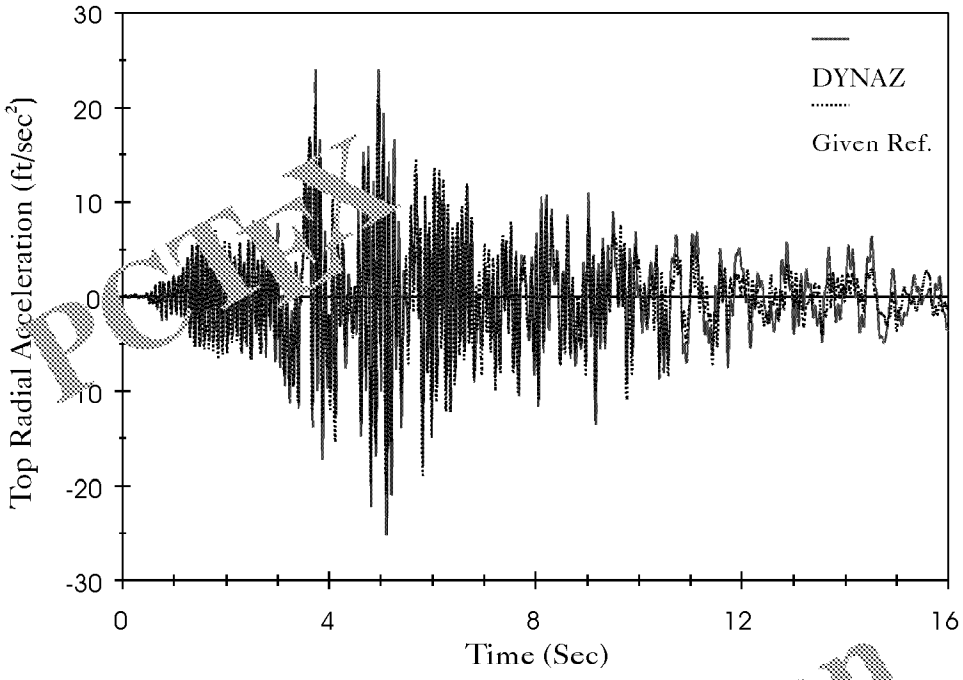

Figure 17: Example 5, Shell Top Horizontal Acceleration

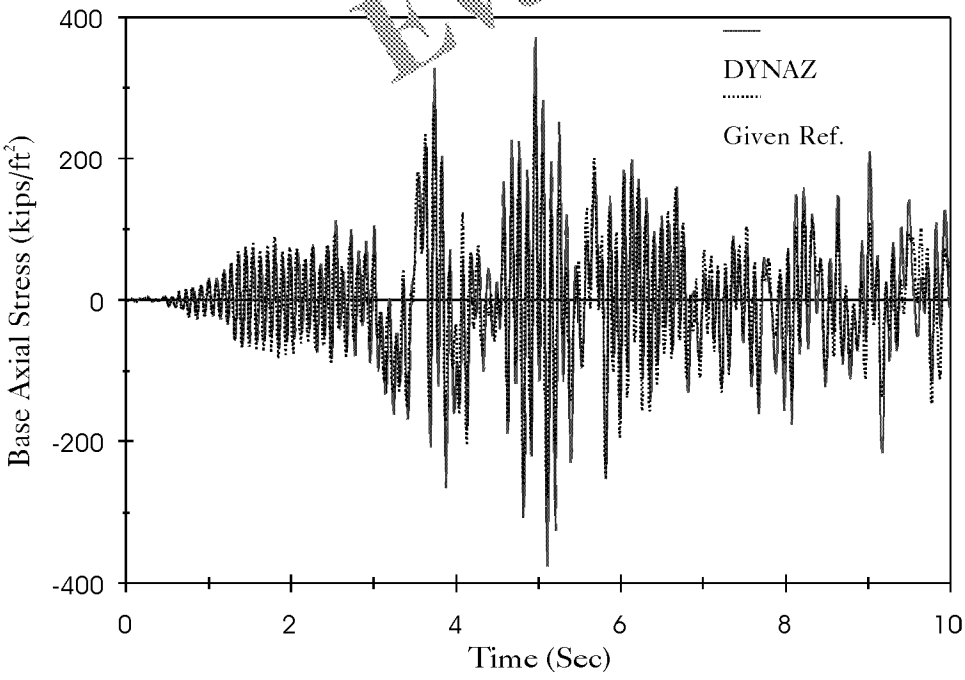

Figure 18: Example 5, Shell Bottom Axial Stress

PCTEL
Evaluation

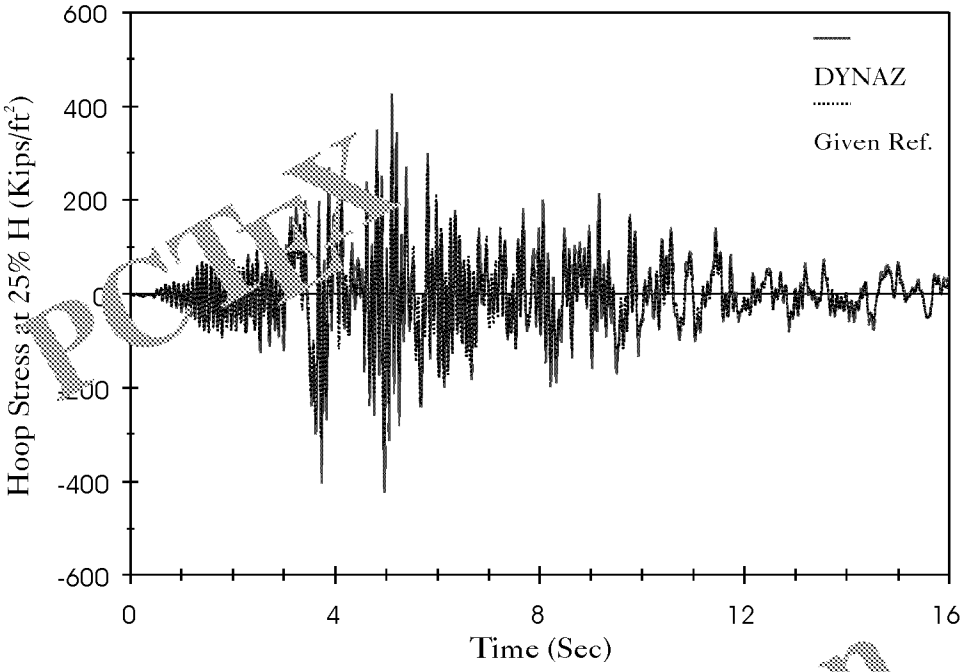

Figure 19: Example 5, Shell Hoop Stress at 25% of the Tank Height

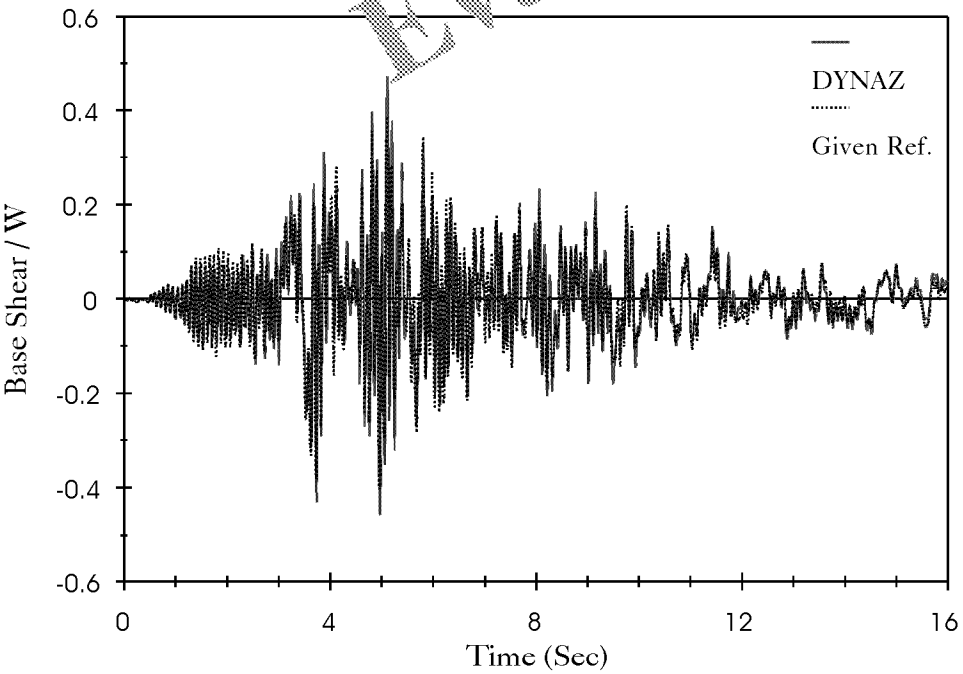

Figure 20: Example 5, Base Shear

PCTRAN Evaluation

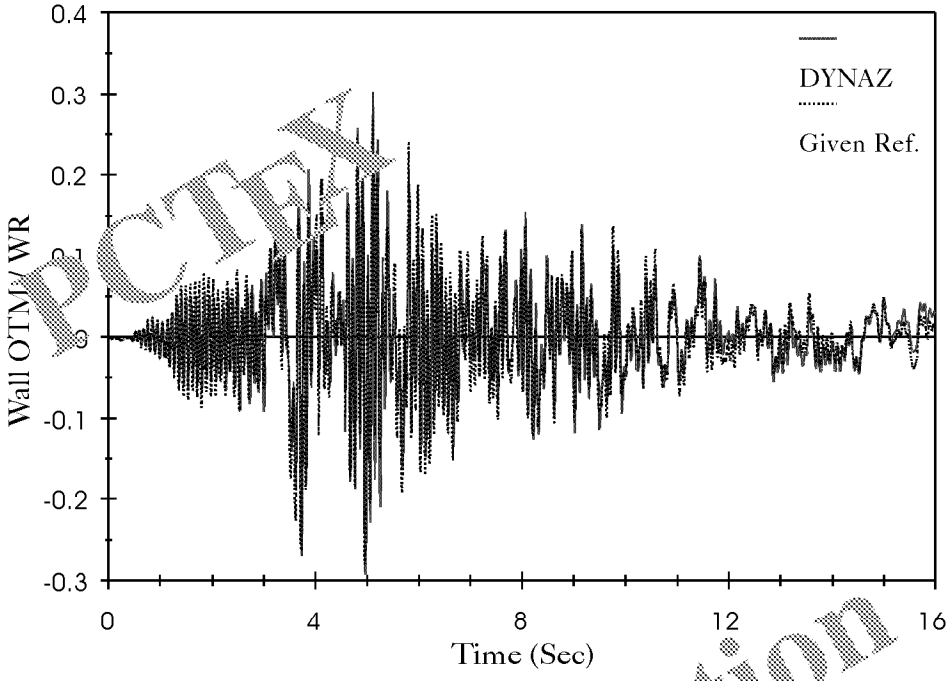

Figure 21: Example 5, Base Overturning Moment

PCTEX Evaluation

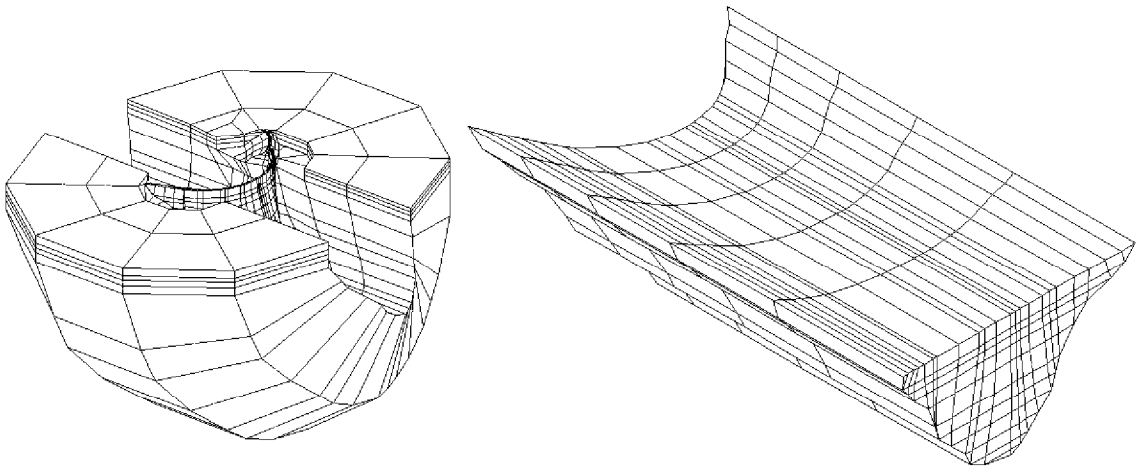

Figure 22: Example 6, Finite Element Model of the Dam, Reservoir and Rock Foundation